Modulation of the Photophysical Properties of 2,2'-Bipyridine-3,3'-diol inside Bile Salt Aggregates: A Fluorescence Based Study for the Molecular Recognition of Bile Salts.

ARTICLE *in* LANGMUIR · DECEMBER 2012

Impact Factor: 4.46 · DOI: 10.1021/la304319r · Source: PubMed

6 AUTHORS, INCLUDING:

Sarthak Mandal
Columbia University
44 PUBLICATIONS **444** CITATIONS
SEE PROFILE

Surajit Ghosh
IIT Kharagpur
45 PUBLICATIONS **381** CITATIONS
SEE PROFILE

Vishal Govind Rao
Bowling Green State University
49 PUBLICATIONS **533** CITATIONS
SEE PROFILE

Nilmoni Sarkar
IIT Kharagpur
159 PUBLICATIONS **3,691** CITATIONS
SEE PROFILE

Langmuir

Article

pubs.acs.org/Langmuir

Modulation of the Photophysical Properties of 2,2′-Bipyridine-3,3′-diol inside Bile Salt Aggregates: A Fluorescence-based Study for the Molecular Recognition of Bile Salts

Sarthak Mandal, Surajit Ghosh, Hari Hara Kumar Aggala, Chiranjib Banerjee, Vishal Govind Rao, and Nilmoni Sarkar*

Department of Chemistry, Indian Institute of Technology, Kharagpur 721302, WB, India

Supporting Information

ABSTRACT: 2,2′-Bipyridine-3,3′-diol ($BP(OH)_2$) has been used as a sensitive excited-state intramolecular proton transfer fluorophore to assess different bile salt aggregates as one of the potential biologically relevant host systems useful for carrying many sparingly water-soluble drug molecules. The formation of inclusion complexes, complex-induced fluorescence behavior, and their binding ability have been investigated from the modulated photophysics of $BP(OH)_2$ by means of photophysical techniques. The constrained hydrophobic environment provided by the aggregates significantly reduces the water-assisted nonradiative decay channels and lengthens the fluorescence lifetime of the proton-transferred DK tautomer. Both the absorption and fluorescence properties of $BP(OH)_2$ are found to be sensitive to the change in the structure, size, and hydrophobicity of the aggregates. Fluorescence quenching experiments were performed to gain insight into the differential distribution of the probe molecules between bulk aqueous phase and nanocavities of various aggregates. The observation of longer fluorescence lifetime and rotational relaxation time in NaDC aggregates compared to that in NaCh and NaTC aggregates indicates that the binding structures of NaDC aggregates are more rigid due to its greater hydrophobicity and larger size and therefore provide better protection to the bound guest. It is noteworthy to mention that the hydrophobic microenvironments provided by bile salt aggregates are much stronger than that provided by micelles and cyclodextrins. The accessibility of water to the aggregate-bound guest can significantly be enhanced with the addition of organic cosolvents. However, the efficiency decreases in the order of dimethylformamide, acetonitrile, and methanol.

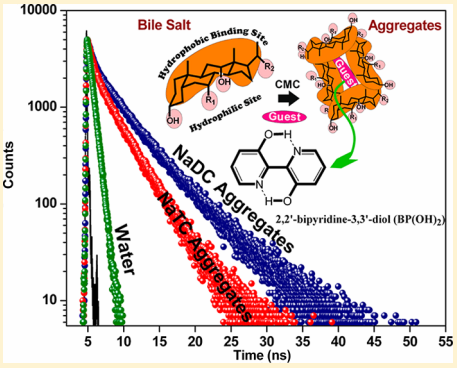

1. INTRODUCTION

Excited-state intramolecular proton transfer (ESIPT) reactions play an important role in various chemical and biological processes[1−3] and consequently find their way in a wide variety of technological applications including the development of proton transfer lasers, white-light-emitting diodes, photostabilizers, and other electronic devices.[4−6] The large Stokes shifted fluorescence emission of the ESIPT chromophores compared to the normal fluorophores helps to improve the fluorescence analyses by avoiding self-absorption or inner filter effect. Most of these molecules have widely been used as a selective fluorophore to probe different biomolecular cavity sites such as micelles, vesicles, proteins, and cyclodextrins as their fluorescence properties are highly sensitive to the change in the surrounding microenvironments.[7−10] Sytnik et al.[8,9] demonstrated how ESIPT chromophores can be utilized in the study of protein conformations and binding site polarity. Several other groups have further demonstrated the greater utility of the ESIPT chromophores in sensing and biological imaging that aims to increase interests in such molecules.[11]

2,2′-Bipyridine-3,3′-diol ($BP(OH)_2$) is such a planar aromatic molecule with two strong intramolecular hydrogen bonds that, on photoexcitation, undergo an excited-state intramolecular double proton transfer (ESIDPT) reaction either in the way of a concerted or stepwise mechanism as shown in Scheme 1. This molecule is of particular interest

Scheme 1. Different Photo-tautomers Involved in the ESIDPT Process of $BP(OH)_2$ Showing the Step-Wise and Concerted Mechanisms

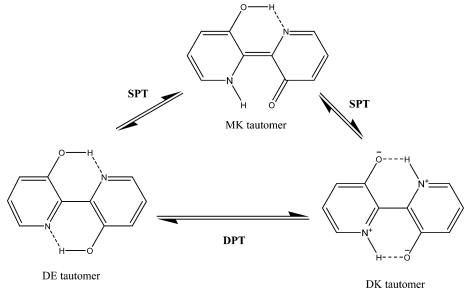

Received: October 31, 2012
Revised: December 7, 2012
Published: December 7, 2012

because of its involvement in the double proton transfer reaction that plays an important role in many real biological systems, for example, in DNA base pairs such as the adenine−thymine base pair, and $BP(OH)_2$ is a representative of such systems[12] similar to a few other ESIPT chromophores such as dimers of 7-azaindole[13−15] and 2-(2′-hydroxyphenyl)-benzoxazole (HBO).[16] The PT process of $BP(OH)_2$ has been well studied both experimentally[17−21] and theoretically[22−25] over the past few decades. It has recently been proposed that both the concerted and sequential pathways may involve simultaneously depending on the nature of the systems and the excitation and emission wavelengths.[26−28] In the concerted mechanism, the PT occurs within the time scale of ∼100 fs as reported on the basis of femtosecond fluorescence upconversion and transient absorption measurements.[29,30] However, in the sequential mechanism of the two-step process, the first step is reported to be ultrafast in nature with the time scale of about 100 fs or less, and the second step that involves the formation of a DK* tautomer from a MK* tautomer occurs in ∼10 ps time regime.

The PT dynamics of $BP(OH)_2$ has been studied extensively in different solvents of varying pH, polarity, and hydrogen-bonding ability.[19,31−34] In solution, the absorption band at ∼340 nm corresponds to the lowest π to π^* transition of the dienol (DE) tautomer.[32] An additional absorption band in the region 400−450 nm has only been observed in aqueous solution due to the stabilization of the DK tautomer in the ground state through water solvation. Such unique spectral behavior in aqueous solution helps to utilize $BP(OH)_2$ as a biomarker and water sensor. The large Stokes-shifted fluorescence emission is attributed to the proton transferred DK* tautomer. Since both the DE and DK tautomers are reported to be very nonpolar with negligible singlet excited-state dipole moments, the position of the absorption and emission maxima are expected to be slightly affected with the change in the polarity of the solvents.[18,21] However, in polar protic solvents, the hydrogen-bonding ability of the solvents largely affects the proton transfer dynamics similar to that observed in a number of other proton transfer probe molecules.[35,36] As the polarity and hydrogen-bonding ability of the protic solvents increases, the blue shift in the emission maxima increases.

Recently, a few studies have been performed demonstrating the caging effect on the absorption and fluorescence properties of $BP(OH)_2$ under the restricted microenvironment of micelles, proteins, and cyclodextrins.[32,37−39] In this manuscript, we have investigated the modulation of ground-state and excited-state properties of $BP(OH)_2$ using bile salt aggregates as potential biologically active host systems. Bile salts are naturally occurring amphiphilic molecules, synthesized from cholesterol within the liver playing the unique role of solubilization of fats and fat-soluble other substances in living organisms.[40,41] The self-assemblies of bile salts are of particular interest because of their better suitability on solubilizing sparingly water-soluble drug molecules over the conventional surfactant forming micelles.[42] Unlike conventional surfactants, bile salts have a nonplanar steroidal skeleton with a convex surface of hydrophobic groups and a concave surface of hydrophilic groups (Scheme 2). The aggregation behavior of bile salt is reported to be complex in nature as its micellar solution exhibits significant polydispersity with respect to the size and structure of the aggregates. Several models have been proposed to explain the aggregation behavior of bile salts in aqueous

Scheme 2. Chemical Structures of Sodium Cholate (NaCh), Sodium Deoxycholate (NaDC), and Sodium Taurocholate (NaTC)

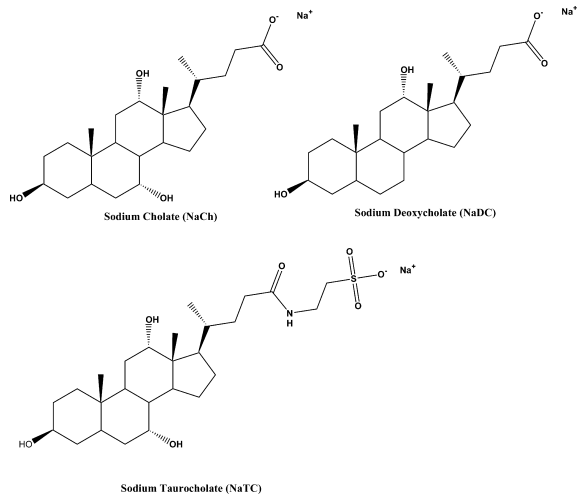

solution. According to the most widely accepted model proposed by Small et al.,[40,43] the primary aggregates consist of 2−10 monomers, where the hydrophilic groups pointed outward are formed at low concentration of bile salt due to the hydrophobic interaction of convex surfaces of monomers. The hydrophobic guest molecules are preferentially solubilized in the hydrophobic nanocavities of primary aggregates. At a higher concentration of bile salts, the primary aggregates are agglomerated to form secondary aggregates of elongated rodlike structure where the hydrophilic probe molecules are preferentially solubilized in the hydrophilic core filled with water. At this high concentration, both the primary and secondary aggregates coexist with two types of binding sites, and the distribution of the primary and secondary aggregates changes as the concentration of bile salt further increases. Although a number of theoretical molecular dynamics simulation[44,45] and experimental studies[46,47] have been performed over the past few decades, the detailed mechanism for the aggregation of bile salts is not yet fully well established. In a recent study, Miranda et al.[48] have shown the utilization of the fluorescent dansyl derivative of cholic acid for the investigation of aggregation behavior of bile salts. Using steady-state and time-resolved fluorescence techniques, they have shown the variation of distribution of primary and secondary aggregates at different concentrations of sodium cholate (NaCh).

Due to the presence of different tunable binding sites, bile salt aggregates are found to be interesting host systems capable of carrying both hydrophobic and hydrophilic guest molecules depending on the structure and size of the guests.[49−54] In recent years, several fluorescent bile acid derivatives have been synthesized through the covalent attachment of small fluorescent molecules to assess their aggregates as an active biological system by means of photophysical techniques.[55,56] Very recently, Zhu and co-workers[57,58] have synthesized a number of cholic acid derivatives to investigate their aggregation behavior and host−guest interaction properties. The incorporation of guests into bile salt aggregates alters the selectivity and kinetics for the photoreactivity of the bound guests.[59,60] While a substantial effort has been made on the study of a number of fluorescence spectroscopy-based photo-

dx.doi.org/10.1021/la304319r | Langmuir 2013, 29, 133−143

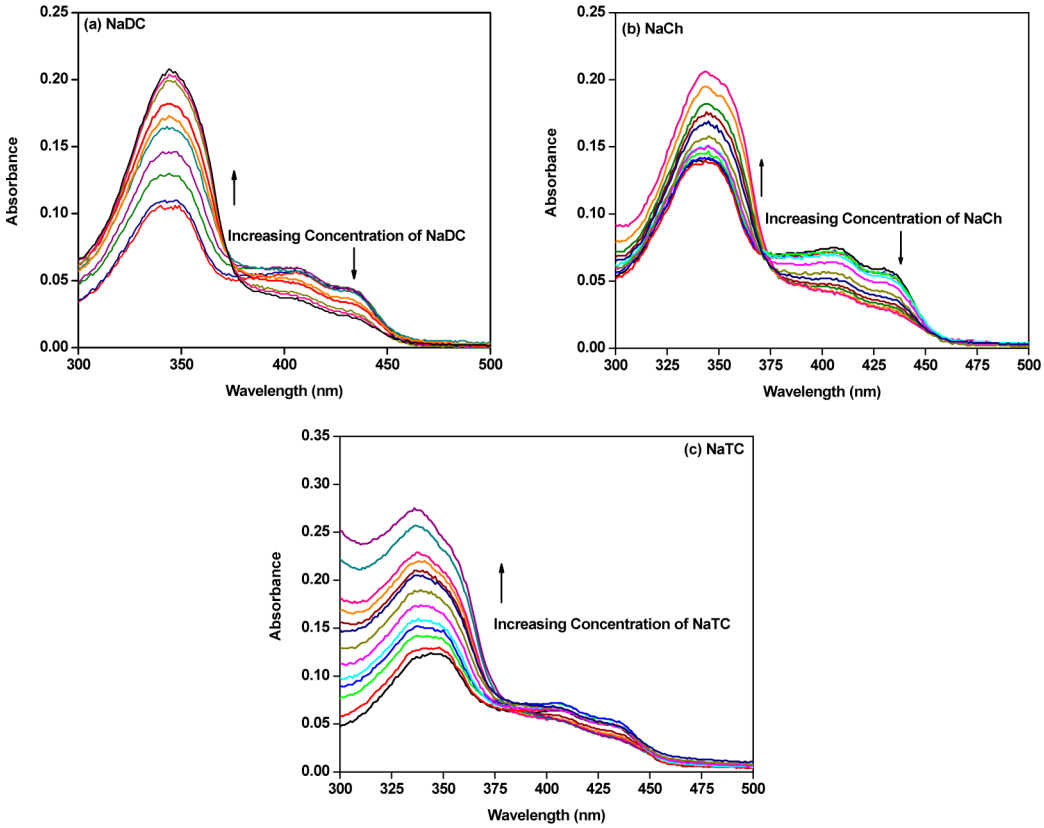

Figure 1. UV−vis absorption spectra of $BP(OH)_2$ in aqueous 0.2 M NaCl solution with increasing concentration of (a) NaDC (0−40 mM), (b) NaCh (0−40 mM), and (c) NaTC (0−40 mM).

physical and dynamical phenomena[61−66] to establish the influence of bile salt aggregates on such alteration, much less attention has been paid on the study of modulating the photophysical properties of ESIPT chromophores, in spite of the fact that most of the applications of the PT chromophores are based on their photophysical properties. Therefore, in the present work, effort has been made on the study of the binding dynamics of $BP(OH)_2$ with three different bile salt aggregates of varying hydrophobicity. It has been found that a minute change in the structural properties of the bile salts largely affects the ground-state and excited-state binding dynamics of the probe molecule. The photophysical behavior of $BP(OH)_2$ has been analyzed over the concentration range 0−40 mM of each bile salt. Since both the DE and DK tautomers are nonpolar in nature with negligible dipole moments, the preferential location of the probe molecules is expected to be in the hydrophobic nanocavities of the primary aggregates even when both the primary and secondary aggregates coexist at a higher concentration of bile salts. Various water-miscible organic cosolvents were employed to accelerate the release of the bound probe molecules to the aqueous phase by making the aggregates less rigid and more accessible to water through the interactions of the cosolvents with bile salt monomers.

2. EXPERIMENTAL SECTION

2.1. Chemicals. 2,2′-Bipyridine-3,3′-diol ($BP(OH)_2$) was used as received from Sigma−Aldrich. The different bile salts, sodium deoxycholate (NaDC), sodium cholate (NaCh), and taurocholate (NaTC), were also purchased from Sigma−Aldrich and used as received. Dimethylformamide (DMF), acetonitrile (ACN), and methanol (MeOH) (spectroscopic-grade; Spectrochem, India) and NaCl (Sigma−Aldrich) were used as received. The structures of all three bile salts used in these experiments are presented in Scheme 2.

2.2. Instruments and Methods. Steady-state absorption and emission spectra were recorded on a Shimadzu (model UV 1601) UV−vis spectrophotometer and a Hitachi (model no. F-7000) spectrofluorimeter, respectively. In all experiments, the concentration of $BP(OH)_2$ was kept $\sim 10^{-5}$ M. Double-distilled Milli-Q water was used to prepare the solutions for experiments. The time-resolved fluorescence lifetime and anisotropy decays were measured with a time-correlated single photon counting (TCSPC) device. The details of the experimental setup for picosecond TCSPC has been described in our previous publication.[67] In brief, a picoseconds diode laser at 375 nm (IBH, UK, Nanoled) was used as the light source, and the signal was detected in magic angle (54.7°) polarization using a Hamamastsu MCP PMT (3809U). The typical instrument response function is ∼100 ps in our system. The decays were analyzed using IBH DAS-6 decay analysis software. The same software was also used for time-resolved anisotropy decay analysis.

For the anisotropy decays, we used a motorized polarizer in the emission side to collect the emission intensities at parallel ($I_\parallel$) and perpendicular ($I_\perp$) polarizations until a certain counts difference between the parallel ($I_\parallel$) and perpendicular ($I_\perp$) decays was reached. The counts difference depends on the tail matching of the parallel ($I_\parallel$) and perpendicular ($I_\perp$) decays.[55] The anisotropy decay function $r(t)$ was constructed from these $I_\parallel$ and $I_\perp$ decays using the following equation:

$$r(t) = \frac{I_\parallel(t) - G \cdot I_\perp(t)}{I_\parallel(t) + 2G \cdot I_\perp(t)} \quad (1)$$

where G is the correction factor for detector sensitivity to the polarization direction of the emission. The G factor was determined following the tail matching procedure as reported in the literature, and the typical value of the G factor for our set up is 0.6.[68]

dx.doi.org/10.1021/la304319r | Langmuir 2013, 29, 133−143

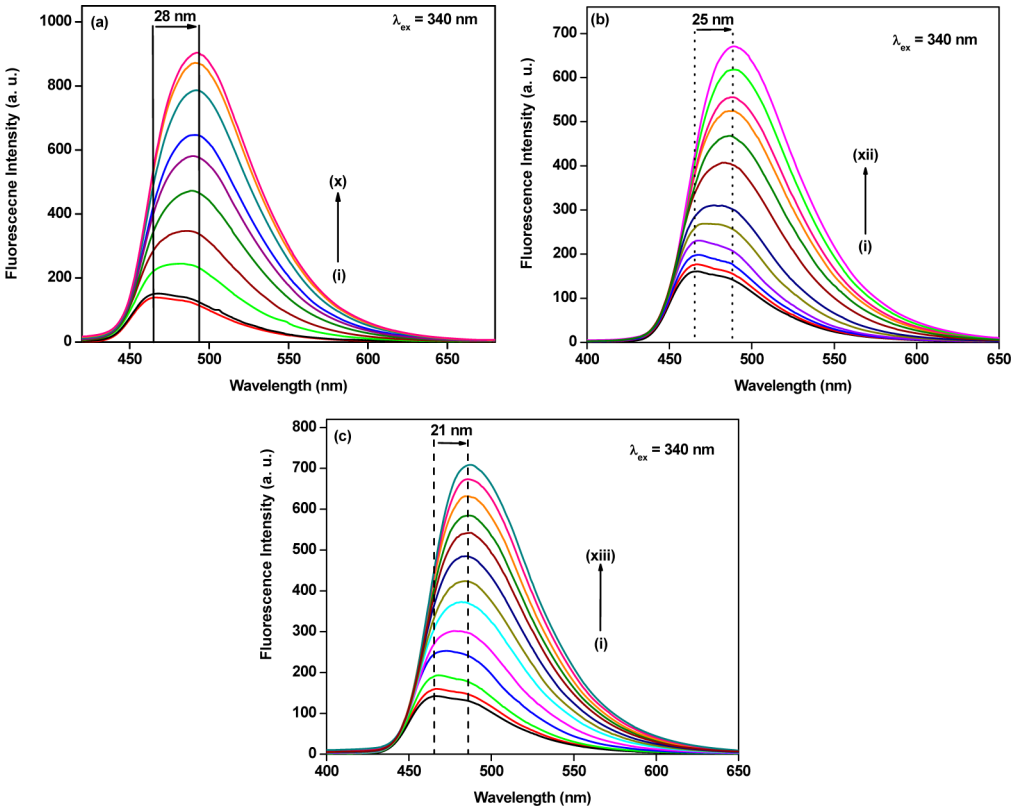

Figure 2. Steady-state fluorescence spectra (λ_{ex} = 340 nm) of $BP(OH)_2$ in aqueous 0.2 M NaCl solution with increasing concentration of (a) NaDC (curves i–x correspond to 0–40 mM NaDC), (b) NaCh (curves i–xii correspond to 0–40 mM NaCh), and (c) NaTC (curves i–xiii correspond to 0–40 mM NaTC).

The fluorescence quantum yields of $BP(OH)_2$ in aqueous solution and in the solution of different bile salt aggregates were determined using anthracene (λ_{abs} = 350 nm) with an absolute quantum yield of 0.27 in ethanol[69] at 25 °C as secondary standard. The following equation was used for calculation:

$$\frac{\Phi_S}{\Phi_R} = \frac{A_S}{A_R} \times \frac{(Abs)_R}{(Abs)_S} \times \frac{n_S^2}{n_R^2} \quad (2)$$

where Φ represents the quantum yield, Abs represents the absorbance, A represents the area under the fluorescence curve, and n is the refractive index of the medium. The subscripts S and R denote the corresponding parameters for the sample and reference, respectively.

2.3. Sample Preparation. Bile salt solutions were prepared by dissolving in aqueous 0.2 M NaCl solution. The stock solutions of bile salts, especially for concentrated solutions, were heated at 50 °C to avoid the probability of gel formation. Now the calculated amount of stock methanolic solution of BP $(OH)_2$ was taken in a volumetric flask so that the ultimate concentration becomes ~10^{-5} M for a specific volume of bile salt solution. After removing the methanol completely, the specific volumes of stock bile salt solutions of varying concentration were added into the flask, and the solutions were kept for few hours for the encapsulation of dye into the microenvironment of the bile salt aggregates.

3. RESULTS AND DISCUSSIONS

3.1. Effect of Structure and Concentration of Bile Salts. *3.1.1. Steady-State Absorption and Fluorescence Studies.* The absorption spectra of $BP(OH)_2$ in aqueous 0.2 M NaCl solution with increasing concentration of different bile salts are shown in Figure 1. As we can see, the addition of bile salts results in an increase in the absorbance at 340 nm with the subsequent decrease in absorbance in the ~400–450 nm region without introducing any significant shift in the absorption maxima of the lowest energy absorption band as expected from the negligible dipole moment of the DE tautomer.[17,21] The increase in absorbance at 340 nm with increasing concentration of bile salts is an indication of forming host–guest inclusion complexes while the decrease in the absorbance in the region 400–450 nm is an indication of lowering the accessibility of water toward the bound guest. The suppression of the red end absorption band with addition of bile salts can be rationalized by the disruption of intermolecular hydrogen-bonded water complexes of the diketo tautomers in the ground state upon confinement. In general, the observation of an isosbestic point is an indication of a simple two-state equilibrium as it has been observed in a conventional surfactant (cationic and nonionic) forming micellar solution.[39] However, no such isosbestic point is observed in the case of binding with bile salt aggregates ruling out the possibility of simple equilibrium between two states. Rather, it implies the binding of the probe molecules in different types of binding sites. This observation is quite expected from the complex aggregation behavior of bile salts. Interestingly, the decrease in absorbance in the 400–450 nm region that indicates the extent of penetration of the probe molecule into the hydrophobic nanocompartment is not so prominent in the case of NaTC aggregates. This differential behavior in NaTC aggregates is probably due to the stronger interaction of the cationic part of the DK tautomer with the negatively charged sulfonate moiety present in the headgroup of NaTC similar to that observed with the headgroup of the anionic surfactant sodium dodecyl sulfate (SDS).[39]

The steady-state fluorescence spectra of $BP(OH)_2$ in the aqueous solution with increasing concentration of different bile

dx.doi.org/10.1021/la304319r | *Langmuir* 2013, 29, 133–143

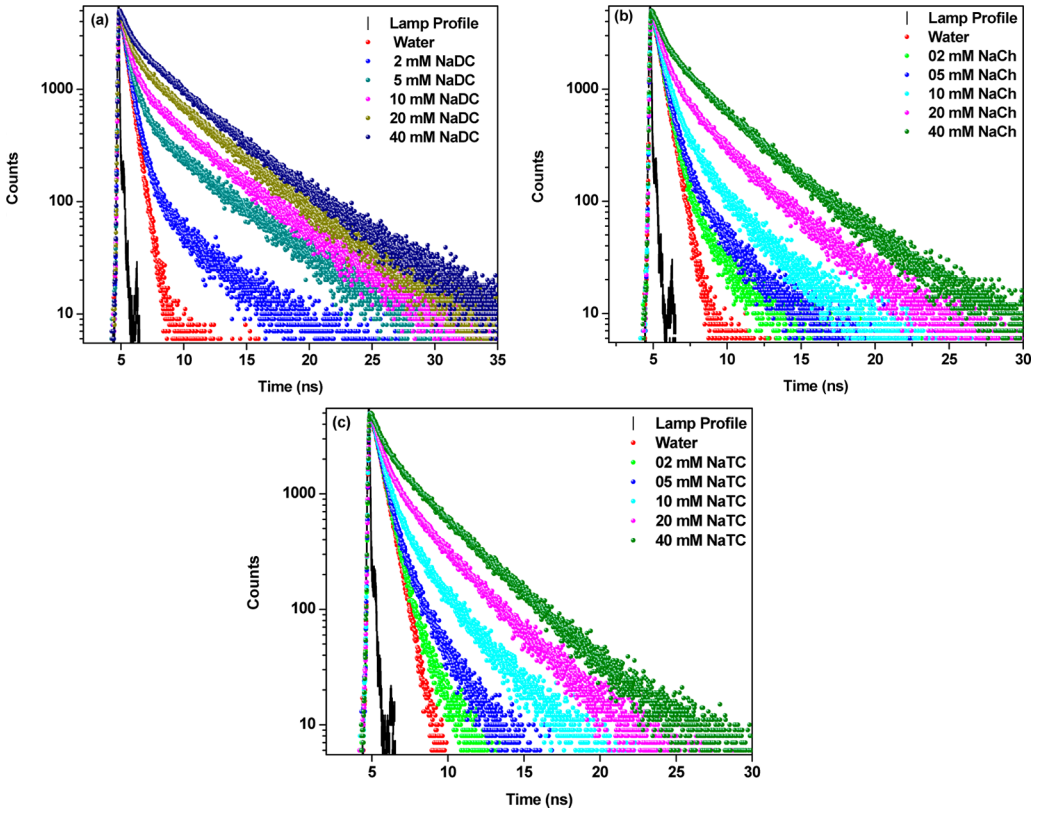

Figure 3. Time-resolved fluorescence decay of $BP(OH)_2$ in aqueous 0.2 M NaCl solutions with an increasing concentration of (a) NaDC, (b) NaCh, and (c) NaTC. (λ_{ex} = 375 nm; λ_{em} = 465 nm).

salts were recorded at the excitation wavelength of 340 nm, and the corresponding changes in the fluorescence behavior have been depicted in Figure 2. The large Stokes-shifted fluorescence is attributed to the double proton transferred DK tautomer. Gradual addition of bile salt leads to the red shift in the emission maxima along with the significant enhancement in emission intensity due to the incorporation of the probe molecules into the hydrophobic binding sites of the primary aggregates. This clearly indicates that the micropolarity sensed by the probe molecules in presence of bile salt aggregates is less than the bulk aqueous phase because comparable red shift in the emission maxima is observed on changing the solvent polarity from water to cyclohexane.[31,32] The emission maxima of $BP(OH)_2$ in NaDC aggregates appear at ~492 nm, which is almost 27 nm red-shifted from water. It is noteworthy to mention that the hydrophobic microenvironment surrounding the probe molecules provided by bile salt aggregates is greater than that provided by cyclodextrins as the emission maxima of $BP(OH)_2$ in bile salt aggregates is found to be more red-shifted than that observed upon binding with cyclodextrin as studied by About-Zied.[32] However, the extent of the red shift is found to be greater in NaDC aggregates followed in order by NaCh and NaTC aggregates (Figure 2) as NaDC aggregates provide relatively more hydrophobic microenvironment. The aggregation behavior of bile salts is largely affected by the change in the structural feature of the bile salts along with the other experimental conditions such as temperature, ionic strength, and pH of the medium. In our earlier publication,[70] we have demonstrated the effect of NaCl on the modulation of the photophysics and photodynamics of another ESIPT probe, 1′-hydrxy-2′-acetonaphtone (HAN), inside various bile salt aggregates. In the present work, we observed an increase in fluorescence intensity with the red shift in the emission maxima of $BP(OH)_2$ upon addition of NaCl due to the enhanced degree of hydrophobicity of the primary binding sites. As the dihydroxy bile salt, NaDC is more hydrophobic compared to the other trihydroxy bile salts, NaCh and NaTC, and the formation of primary aggregates is reported to be governed by hydrophobic interactions, the onset aggregation occurs at a lower monomer concentration for NaDC followed in order by NaCh and NaTC under the same experimental condition.[41,45] This can be supported from our experimental observations that the spectral alteration of $BP(OH)_2$ appears at a lower concentration of bile salt monomers for the binding with NaDC aggregates than NaCh and NaTC aggregates as clearly observed from the change in emission maxima of $BP(OH)_2$ as a function of bile salt concentration. In each plot of emission maxima versus concentration (Figure S1, Supporting Information), a point of inflection is observed at the critical micelle concentration (cmc) for the formation of primary aggregates of the corresponding bile salts. The cmc values thus obtained are in good agreement with the reported cmc values in the literature. With increasing concentration of bile salts, the quantum yield increases (Figure S2, Supporting Information), and finally, at higher concentration, it ensures the saturation of host−guest interactions. For the three different bile salts of varying hydrophobicity, the maximum enhancement of fluorescence efficiency is observed upon incorporation into the NaDC aggregates. This work therefore demonstrates that a slight difference in the chemical properties of the host systems can bring large difference in the partitioning of hydrophobic probe molecules into their cavities.

3.1.2. Time-Resolved Fluorescence Studies. Fluorescence lifetime measurements provide valuable information about the

dx.doi.org/10.1021/la304319r | *Langmuir* 2013, 29, 133−143

binding and location of the probe molecules in bile salt aggregates because the excited-state interactions of $BP(OH)_2$ are strongly affected by the change in the surrounding microenvironments. In this work, we have recorded the fluorescence decays of $BP(OH)_2$ in aqueous solution of three different bile salts with increasing concentration at the excitation and emission wavelengths of 375 and 465 nm, respectively (Figure 3). In aqueous solution, the decay fits well to a biexponential function with the time constants ~0.54 and 5.48 ns that are consistent with the literature report.[31] The fast component is assigned to the intramolecularly hydrogen-bonded DK tautomer (dizwitterionic) that is stabilize by the interaction of water with its polar parts. The longer lifetime component of 5.48 ns, although less in percent of contribution, arises from the intermolecularly hydrogen-bonded rigid water complex of the DK tautomer as described by Abou-Zied.[32] By the term rigid water complex, they meant to say that the rotation of the intermoleculary hydrogen-bonded water complex of the DK* tautomer is prohibited by the rigid hydrogen-bonded network of the water molecules resulting in a longer lifetime component.

In the presence of bile salts, a longer lifetime component is observed along with the fast component (0.54 ns) that is observed in pure water (Table 1). The longer lifetime component arises from the aggregates bound $BP(OH)_2$. When the probe molecules are preferentially incorporated into the hydrophobic nanocavities of the primary aggregates, the accessibility of water toward the probe molecules becomes restricted resulting in the effective decrease of the water-assisted nonradiative decay channels to enhance fluorescence lifetime of the bound guest. The relative contribution of the longer lifetime component (a_2), which roughly corresponds to the fraction of the guest that is incorporated into the bile salt aggregates, increases gradually as the concentration of the bile salt increases (Table 1) with the commitment decrease in the relative contribution of the fast component responsible for the free $BP(OH)_2$ present in the aqueous phase. At a particular concentration of bile salt, for example, at 40 mM concentration of bile salt, the relative contribution of the longer lifetime component, which is attributed to the aggregates bound probe molecules, is found to be greater in the case of binding with NaDC aggregates compared to NaCh and NaTC aggregates. This corresponds to higher encapsulation efficiency of $BP(OH)_2$ in NaDC aggregates resulting from the introduction of greater hydrophobic microenvironment to the bound guest that in turn helps to enhance the solubilization of the nonpolar probe molecule and consequently the partitioning of the $BP(OH)_2$. Moreover, when the relative amplitudes of the fast and slow decay components were plotted as a function of concentration for the three different bile salts, the higher encapsulation of the probe molecules into the NaDC aggregates became evident from the comparatively sharp decrease in the contribution of the fast component with concentration (Figure S3, Supporting Information).

Table 1. Fluorescence Lifetime and Quantum Yield (Φ_f) of $BP(OH)_2$ in Aqueous 0.2 M NaCl Solution with Increasing Concentration of Bile Salt

bile salt	conc/mM	τ_1/ns (a_1)	τ_2/ns (a_2)	$\langle\tau_f\rangle^a$/ns	Φ_f
	0	0.53 (0.99)	5.48 (0.01)	0.6	0.078
	2	0.55 (0.98)	4.13 (0.02)	0.6	0.106
	5	0.57 (0.89)	4.77 (0.11)	1.0	0.155
NaDC	10	0.58 (0.80)	4.79 (0.20)	1.4	0.235
	20	0.63 (0.68)	4.80 (0.32)	2.0	0.280
	40	0.75 (0.54)	4.91 (0.46)	2.7	0.330
	2	0.53 (0.98)	2.98 (0.02)	0.6	0.087
	5	0.56 (0.96)	2.88 (0.04)	0.7	0.095
	10	0.57 (0.89)	2.80 (0.11)	0.8	0.130
NaCh	20	0.63 (0.80)	3.56 (0.20)	1.2	0.210
	40	0.69 (0.62)	3.84 (0.38)	1.9	0.250
	2	0.61 (0.96)	1.70 (0.04)	0.7	0.084
	5	0.59 (0.91)	1.98 (0.09)	0.7	0.092
	10	0.60 (0.86)	2.68 (0.14)	0.9	0.135
NaTC	20	0.60 (0.75)	3.12 (0.25)	1.2	0.180
	40	0.65 (0.58)	3.44 (0.42)	1.8	0.192

$^a\langle\tau_f\rangle = a_1\tau_1 + a_2\tau_2$ for biexponential fluorescence decays where τ_1 and τ_2 are the lifetime components with their corresponding relative amplitudes a_1 and a_2; experimental error ±5%.

For the three different bile salts of concentration 40 mM, the average fluorescence lifetime is found to be greater in NaDC aggregates compared to those in NaCh and NaTC indicating the highest degree of incorporation of $BP(OH)_2$ in NaDC aggregates (Figure S4, Supporting Information). This trend is in complete agreement with that which is observed in the steady-state fluorescence measurement. This is an outcome of the fact that NaDC aggregates provide better protection of the bound guest from the interaction of water resulting in a effective decrease of the water-assisted nonradiative decay rate and the magnitude of which is found to be more efficient in NaDC aggregates. Slight variation of the fluorescence lifetime values particularly the values of the longer lifetime component above cmc is observed probably due to the binding of the probe molecules in different microenvironments of primary/secondary aggregates. By means of photophysical technique, recently, Miranda et al.[48] have shown that the secondary aggregates start to appear at 10 mM concentration of NaCh. However, below 25 mM concentration, primary aggregates predominant over the secondary aggregates. Moreover, the increase in the lifetime values of the longer lifetime component with increasing concentration can be explained on the basis of the increased size of the aggregates. In addition to that, at higher bile salt concentration, the viscosity of the solution increases more effectively for the NaDC aggregates than for the NaCh and NaTC aggregates resulting in the slight increase in fluorescence lifetime of the fast component that corresponds to the free $BP(OH)_2$ present in the aqueous phase.

The presence of the probe molecules in the bulk aqueous phase and in the aggregated phase was further confirmed by monitoring the time-resolved fluorescence decays at different emission wavelengths. As the monitoring emission wavelength changes from the blue end (465 nm) to the red end (525 nm) of the steady-state emission spectra, the contribution of the longer lifetime components increases without any significant change in the lifetime values (Table S1, Supporting Information). This indicates that the longer lifetime component is responsible for the probe molecules present inside the bile salt aggregates.

3.1.3. Time-Resolved Fluorescence Anisotropy Studies. In the preceding sections, clearly, we have an idea about the extent of binding and the location of the probe molecules from the steady-state and time-resolved fluorescence decay measurements. However, to obtain a better insight into the microenvironment around the bound guests, time-resolved fluorescence anisotropy measurements of $BP(OH)_2$ in the aqueous

dx.doi.org/10.1021/la304319r | Langmuir 2013, 29, 133−143

solution of different bile salts were performed using a picoseconds time-correlated single photon counting (TCSPC) device. It furnishes the valuable information regarding the rotational motion of the probe molecules in such restricted microenvironments. Previously, Glasbeek and co-workers[28] studied the femtosecond fluorescence anisotropy of $BP(OH)_2$ in solutions of aprotic solvents acetonitrile and cyclohexane. They found an ultrafast anisotropy decay component of 350 fs when monitored at the blue end (460 nm) of the broad emission spectra of $BP(OH)_2$. This ultrafast component is attributed to the dienol tautomer of $BP(OH)_2$. The additional picosecond components with time constants of 10 ps and 20−40 ps are responsible for the transformation of the MK* to DK* and the rotational motion of the DK* in solution, respectively. However, the present work mainly deals with the rotational motion of the relaxed excited-state species generated after the ultrafast ESIPT process as we report on the photophysical properties of $BP(OH)_2$ in the picosecond time scale. So far, there is no study on the rotational motion of this probe molecule inside the restricted microenvironments of chemical and biological nanocavities. The anisotropy decays of $BP(OH)_2$ in bile salt aggregates are found to be biexponential in nature with two time constants; one is in the picoseconds time scale while the other one is in the nanosecond time scale (Figure 4 and Table 2). These components are representative

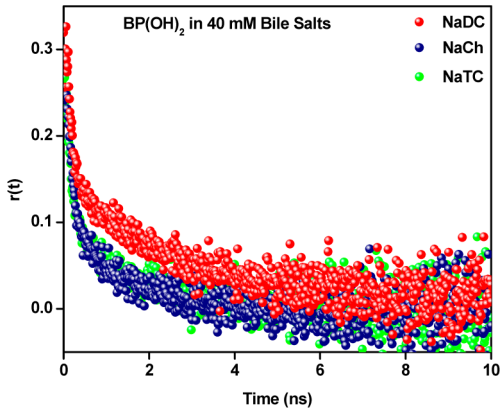

Figure 4. Fluorescence anisotropy decays of $BP(OH)_2$ in aqueous 0.2 M NaCl solution of 40 mM NaDC (red), NaCh (navy blue), and NaTC (green). (λ_{ex} = 375 nm; λ_{em} = 490 nm).

Table 2. Dynamic Parameters of Fluorescence Anisotropy of $BP(OH)_2$ in Aqueous 0.2 M NaCl Solution of Different Bile Salt Aggregates

system	conc/mM	a_{1r}	τ_{1r}/ns	a_{2r}	τ_{2r}/ns	$\langle\tau_r\rangle^a$/ns	χ^2
NaDC	40	0.42	0.12	0.58	2.41	1.5	1.01
NaC	40	0.61	0.14	0.39	1.63	0.7	1.03
NaTC	40	0.60	0.13	0.40	1.59	0.7	1.00

$^a\langle\tau_r\rangle = a_{1r}\tau_{1r} + a_{2r}\tau_{2r}$ where τ_{1r} and τ_{2r} are two rotational relaxation time constants and a_{1r} and a_{2r} are their relative amplitudes, respectively; experimental error ±5%.

of the influence of rotational diffusion motions of the probe molecules partitioned in water and in the hydrophobic nanocavities of bile salt aggregates. The observation of longer rotational relaxation time constants indicates that the probe molecules are located in a motionally restricted microenvironment of bile salt aggregates. The longer rotational relaxation time in NaDC aggregates is found to be almost 1.5 times that observed in the NaCh and NaTC aggregates. This indicates that $BP(OH)_2$ experiences a comparatively more rigid microenvironment in the NaDC aggregates than in the NaCh and NaTC aggregates. However rotational relaxation time constants are found to be almost identical in the NaCh and NaTC aggregates. Therefore, the structural features of the bile salts play an important role in controlling the binding dynamics of the guest in their aggregates. Several experimental studies have shown that the size of the NaDC aggregates are comparatively larger than the NaCh and NaTC aggregates, which further explains the observation of higher rotational relaxation time constants when $BP(OH)_2$ is bound to the NaDC aggregates.[49,60]

3.1.4. Steady-State and Time-Resolved Fluorescence Quenching Study. Steady-state and time-resolved fluorescence quenching experiments were performed using iodide ions as the quencher to get a better insight into the location of the probe molecules inside the bile salt aggregates. The concentration of 40 mM bile salts has been chosen because at this concentration the host−guest interactions become saturated. The ionic quencher iodide is known to quench the singlet excited-state fluorescence properties of the probe molecules in water as well as in presence of bile salt aggregates.[49−52] However, the quenching efficiency depends upon the accessibility of the quencher toward the guest molecules, which further depends on the protection efficiency of the host systems. The greater is the accessibility, the lesser will be the efficiency of the host system to protect the probe molecules and as a consequence the greater will be the quenching efficiency. The idea is that the negatively charged iodide quencher is highly water-soluble and is expected to be present in the polar aqueous phase not inside the hydrophobic interior of bile salt aggregates because of weak interactions with the negatively charged bile salt monomers. The steady-state fluorescence quenching of $BP(OH)_2$ with the addition of NaI has been followed using the following Stern−Volmer equation:

$$\frac{F_0}{F} = 1 + K_{SV}[Q] \tag{3}$$

where I_0 and I are the emission intensities of $BP(OH)_2$ in the absence of quencher and in presence of quencher, respectively. [Q] is the concentration of quencher (NaI), and K_{SV} is the Stern−Volmer quenching constant. The Stern−Volmer quenching plots (Figure 5a) are found to be linear for all the systems indicating only one type of quenching. The slope of each plot provides the Stern−Volmer quenching constants (K_{SV}). From the experimental results, we have found that the quenching is very much faster in aqueous solution when the probe molecules are free to move compared to that when it is bound to the primary aggregates. For the three different bile salt aggregates, the Stern−Volmer constants decrease in the order NaDC (1.46 M^{-1}) < NaCh (2.92 M^{-1}) < NaTC (3.19 M^{-1}), in complete agreement with that expected from encapsulation efficiency of the probe molecules into the different aggregates. However to be sure about the occurring of only dynamical quenching and no static quenching, we have performed time-resolved fluorescence quenching of $BP(OH)_2$ (Figure S5, Supporting Information) with the addition of NaI and found linear S−V plots (Figure 5b). Moreover, the steady-state fluorescence intensity ratios (F_0/F) are found to be almost equal to the average fluorescence lifetime ratios τ_0/τ for the quenching of $BP(OH)_2$ by NaI in the aqueous solution of all the three bile salt aggregates (Figure S6, Supporting

dx.doi.org/10.1021/la304319r | Langmuir 2013, 29, 133−143

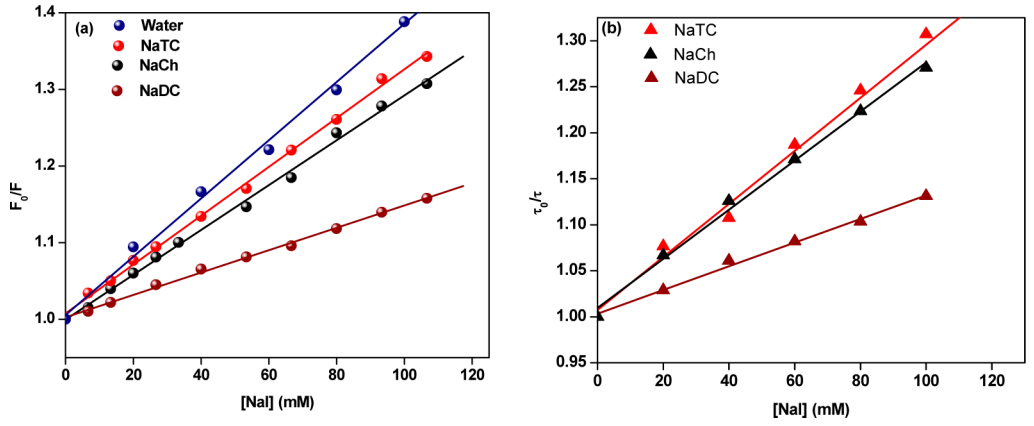

Figure 5. Stern–Volmer plots for (a) steady-state and (b) time-resolved fluorescence quenching of $BP(OH)_2$ in aqueous 0.2 M NaCl solution of different bile salt aggregates by sodium iodide quencher.

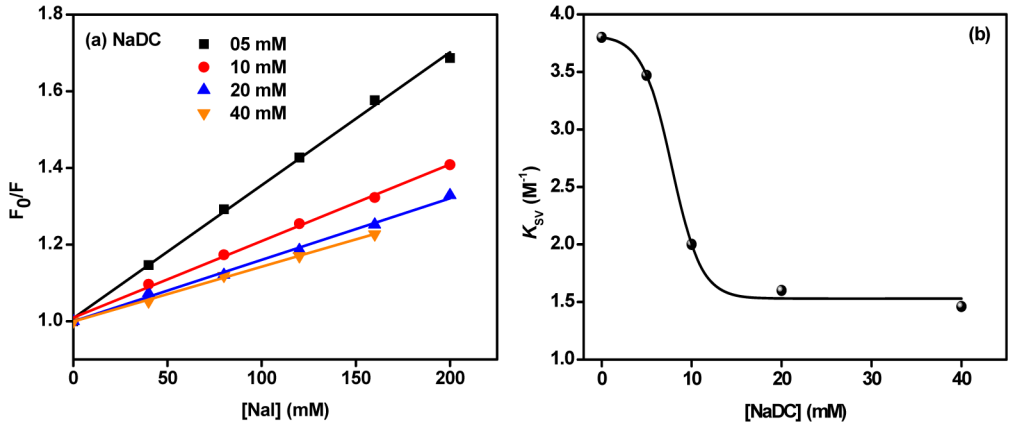

Figure 6. (a) S–V plot for the steady-state fluorescence quenching of the $BP(OH)_2$ in the presence of different concentrations of NaDC bile salt. (b) Dependence of Stern–Volmer quenching constant values with concentration of NaDC.

Information). This observation further strengthens the occurrence of only dynamic quenching and no static quenching. We have also performed the steady-state and time-resolved fluorescence quenching of the probe molecules at various concentration of bile salt taking NaDC as a representative example. The values of Stern–Volmer quenching constants in the presence of NaDC over the concentration range 0–40 mM were obtained from the slope of the linear S–V quenching plots (Figure 6a). The onset concentration at which the protection of the guest molecules starts to appear that further implies the formation of primary aggregates is indicated from the sharp decrease of the K_{SV} values with increasing concentration of NaDC (Figure 6b).

3.2. Effect of Organic Cosolvents on NaDC Aggregates. So far, we have successfully demonstrated that the fluorescence properties of $BP(OH)_2$ are highly sensitive to the structure and dynamics of the bile salt aggregates in which it is confined. The size, shape, and hydrophobicity of the aggregates are the key factors in controlling the binding efficiency, location, and dynamics of the probe molecules as well as the protection efficiency to protect against the excited-state quenching by an external quencher. Recently, it has been shown that the addition of a water-miscible organic cosolvent such as DMF and acetonitrile can significantly modulate the binding dynamics and residence time of the confined probe in cholate aggregates (40 mM).[70,71] Therefore, in the present work, we have attempted to draw a comparative study by elucidating the effect of three different cosolvents, DMF, acetonitrile, and methanol, on NaDC aggregates taking $BP(OH)_2$ as a sensitive molecular reporter. Steady-state and time-resolved fluorescence experiments were performed to monitor the changes in the surrounding microenvironment of the probe molecule upon the addition of cosolvents. The changes in the fluorescence spectra with increasing mole fraction of DMF are given in Figure 7a as a representative example whereas the other figures for the addition of MeOH and ACN are given in the Supporting Information (Figure S7). As we can see, the addition of cosolvents results in a decrease of fluorescence intensity with the significant blue shift in the emission maxima indicating more a hydrophilic environment surrounding the probe molecule than that was present before the addition of cosolvent. Figure 7c,d is given for the better understanding of the change in intensity at 492 nm and emission maxima as a function of increasing mole fraction of various cosolvents. Our results show that effectiveness of the cosolvent in bringing the probe molecules out of the cavity sites (as evident from the decrease in fluorescence intensity) through the perturbation of the aggregates follows the trend DMF > ACN > MeOH. Moreover, the extent of blue shift in the emission maxima is found to be greater with the addition of DMF and then followed in order by acetonitrile and methanol. Basically, cosolvents make the binding site less rigid and more polar, that is, more accessible to water through interaction with bile salt monomers. DMF molecules by virtue of their strong

dx.doi.org/10.1021/la304319r | *Langmuir* 2013, 29, 133–143

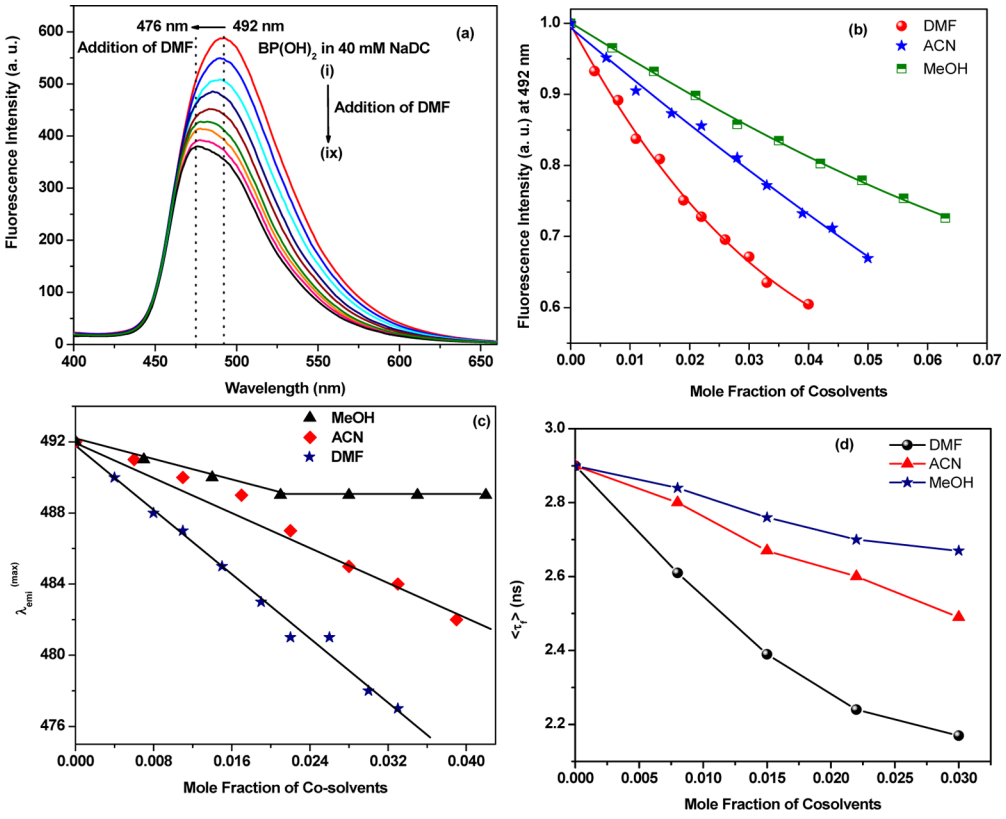

Figure 7. Change in (a) fluorescence spectra of $BP(OH)_2$ with increasing mole fraction of DMF (0–0.04), (b) fluorescence intensity at 492 nm, (c) steady-state fluorescence emission maxima, and (d) average fluorescence lifetime with increasing mole fraction of DMF, acetonitrile, and methanol in aqueous solution of 40 mM NaDC.

hydrogen-bonding ability interact with the bile salt monomers more effectively than acetonitrile and methanol and therefore enhance the water accessibility to the binding site in a greater extent. Between methanol and acetonitrile, acetonitrile is more effective in bringing the changes in the fluorescence of $BP(OH)_2$. Here, the microscopic structure of the water–cosolvent binary mixture at low mole fraction of cosolvent plays an important role in controlling the influence of cosolvent on bile salt aggregates. Wakisaka et al.[72] pointed out that the interaction of water with methanol in the microscopic level is quite different from that of acetonitrile. The difference comes from the fact that the OH group of methanol can act as both a hydrogen-bond donor and acceptor while the CN group of ACN acts as only a hydrogen-bond acceptor. As a matter of fact, the hydrogen-bonding network of water can easily be substituted by methanol while it is difficult by acetonitrile. Therefore, acetonitrile molecules are expected to be more available to interact with bile salt monomers to affect the aggregated structure as it does by DMF however more effectively. The decrease in fluorescence lifetime follows the same trend (Figure 7d) as it follows for the decrease in steady-state fluorescence intensity with the addition of cosolvents. Addition of DMF results in the decrease in the relative contribution (a_2) of the longer lifetime component (Figure S8, Supporting Information) more effectively than acetonitrile and methanol.

4. CONCLUSION

The present work therefore successfully demonstrates the modulation of the ground- and excited-state properties of $BP(OH)_2$ upon confinement into the hydrophobic nanocavities of three different bile salt aggregates of varying hydrophobicity (NaDC/NaCh/NaTC). It has been found that a minute change in the structural features of bile salts largely affects the binding dynamics of the confined probe molecule. The more rigid and hydrophobic NaDC aggregates provide better protection to the bound guests from the interaction with water as evident from much longer fluorescence lifetime and rotational relaxation time for the caged tautomer of $BP(OH)_2$ in NaDC compared to those in NaCh and NaTC. The observation of higher encapsulation efficiency and lesser extent of collisional quenching of $BP(OH)_2$ in NaDC aggregates compared to those in the NaCh and NaTC aggregates further supports the above inference. This work further demonstrates the cosolvent-induced release of the aggregates bound probe molecules due to the enhanced accessibility of water to the binding site results from the interaction of cosolvents with bile salt monomers. However, among the cosolvents used, DMF is found to be more effective than acetonitrile in bringing the probe molecules out of the cavity sites.

■ ASSOCIATED CONTENT

Supporting Information

Information on the additional quantum yield plot, lifetime and pre-exponential factor values, change in the emission maxima with bile salt concentration, time-resolved fluorescence decays of $BP(OH)_2$ with addition of NaI, and cosolvent effects. This material is available free of charge via the Internet at http://pubs.acs.org.

dx.doi.org/10.1021/la304319r | *Langmuir* 2013, 29, 133–143

AUTHOR INFORMATION

Corresponding Author

*E-mail: nilmoni@chem.iitkgp.ernet.in; fax: 91-3222-255303.

Notes

The authors declare no competing financial interest.

ACKNOWLEDGMENTS

N.S. is thankful to Council of Scientific and Industrial Research (CSIR), Government of India, for generous research grants. S.M., S.G., and V.G.R. are thankful to CSIR for a research fellowship. C.B. is thankful to UGC for a research fellowship.

REFERENCES

(1) Zhong, D.; Douhal, A.; Zewail, A. H. Femtosecond Studies of Protein−Ligand Hydrophobic Binding and Dynamics: Human Serum Albumin. *Proc. Natl. Acad. Sci. U.S.A.* **2000**, *97*, 14056−14061.

(2) Chattoraj, M.; King, B. A.; Bublitz, G. U.; Boxer, S. G. Ultra-fast Excited State Dynamics in Green Fluorescent Protein: Multiple States and Proton Transfer. *Proc. Natl. Acad. Sci. U.S.A.* **1996**, *93*, 8362−8367.

(3) Miskovsky, P. Hypericin - A New Antiviral and Antitumor Photosensitizer: Mechanism of Action and Interaction with Biological Macromolecules. *Curr. Drug Targets* **2002**, *3*, 55−84.

(4) Service, R. F. Organic LEDs Look Forward to a Bright, White Future. *Science* **2005**, *310*, 1762−1763.

(5) Parthenopoulos, D. A.; McMorrow, D. P.; Kasha, M. Comparative Study of Stimulated Proton-Transfer Luminescence of Three Chromones. *J. Phys. Chem.* **1991**, *95*, 2668−2674.

(6) Haddon, R. C.; Stillinger, F. H. *Molecular Electronic DeVices*; Carter, F. L., Ed.; Marcel Dekker: New York, 1987.

(7) Catalán, J.; Valle, J. C. D.; Diaz, C.; Palomar, J.; Paz de, J. L. G.; Kasha, M. Solvatochromism of Fluorophores with an Intramolecular Hydrogen Bond and Their Use as Probes in Biomolecular Cavity Sites. *Int. J. Quantum Chem.* **1999**, *72*, 421−438.

(8) Sytnik, A.; Gormin, D.; Kasha, M. Interplay between Excited-State Intramolecular Proton Transfer and Charge Transfer in Flavonols and Their Use as Protein-Binding-Site Fluorescence Probes. *Proc. Natl. Acad. Sci. U.S.A.* **1994**, *91*, 11968−11972.

(9) Sytnik, A.; Litvinyuk, I. Energy Transfer to a Proton-Transfer Fluorescence Probe: Tryptophan to a Flavonol in Human Serum Albumin. *Proc. Natl. Acad. Sci. U.S.A.* **1996**, *93*, 12959−12963.

(10) Mandal, S.; Rao, V. G.; Ghatak, C.; Pramanik, R.; Sarkar, S.; Sarkar, N. Photophysics and Photodynamics of 1′-Hydroxy-2′-acetonaphthone (HAN) in Micelles and Nonionic Surfactants Forming Vesicles: A Comparative Study of Different Microenvironments of Surfactant Assemblies. *J. Phys. Chem. B* **2011**, *115*, 12108−12119.

(11) Zhao, J.; Ji, S.; Chen, Y.; Guo, H.; Yang, P. Excited State Intramolecular Proton Transfer (ESIPT): From Principal Photophysics to the Development of New Chromophores and Applications in Fluorescent Molecular Probes and Luminescent Materials. *Phys. Chem. Chem. Phys.* **2012**, *14*, 8803−8817.

(12) Abou-Zied, O. K. Examining [2,2′-Bipyridyl]-3,3′-diol as a Possible DNA Model Base Pair. *J. Photochem. Photobiol. A* **2006**, *182*, 192−201.

(13) Douhal, A.; Kim, S. K.; Zewail, A. H. Femtosecond Molecular Dynamics of Tautomerization in Model Base Pairs. *Nature* **1995**, *378*, 260−263.

(14) Chen, Y.; Gai, F.; Petrich, J. W. Solvation of 7-Azaindole in Alcohols and Water: Evidence for Concerted, Excited-State, Double-Proton Transfer in Alcohols. *J. Am. Chem. Soc.* **1993**, *115*, 10158−10166.

(15) Takeuchi, S.; Tahara, T. Femtosecond Ultraviolet−Visible Fluorescence Study of the Excited-State Proton-Transfer Reaction of 7-Azaindole Dimer. *J. Phys. Chem. A* **1998**, *102*, 7740−7753.

(16) Ogawa, A. K.; Abou-Zied, O. K.; Tsui, V.; Jimenez, R.; Case, D. A.; Romesberg, F. E. A Phototautomerizable Model DNA Base Pair. *J. Am. Chem. Soc.* **2000**, *122*, 9917−9920.

(17) Bulska, H. Intramolecular Cooperative Double Proton Transfer in [2,2′-Bipyridyl]-3,3′-diol. *Chem. Phys. Lett.* **1983**, *98*, 398−402.

(18) Sepiol, J.; Bulska, H.; Grabowska, A. The Dihydroxy Derivative of 2,2′-Bipyridyl as a New Proton-Transfer Lasing Dye. *Chem. Phys. Lett.* **1987**, *140*, 607−610.

(19) Sepiol, J.; Grabowska, A.; Bulska, H.; Mordzinski, A.; Perez Salgado, F.; Rettschnick, R. P. H. The Role of the Triplet State in Depopulation of the Electronically Excited Proton-Transferring System [2,2′-Bipyridyl]-3,3′-diol. *Chem. Phys. Lett.* **1989**, *163*, 443−448.

(20) Wortmann, R.; Elich, K.; Lebus, S.; Liptay, W.; Borowicz, P. Electrooptical Absorption Measurements of Phototautomerizing Systems: S_0 and S_1 Static Polarizabilities of Bipyridinediols. *J. Phys. Chem.* **1992**, *96*, 9724−9730.

(21) Borowicz, P.; Grabowska, A.; Wortmann, R.; Liptay, W. Tautomerization in Fluorescent States of Bipyridyl-diols: A Direct Confirmation of the Intramolecular Double Proton Transfer by Electro-optical Emission Measurements. *J. Lumin.* **1992**, *52*, 265−273.

(22) Ortiz-Sánchez, J. M.; Gelabert, R.; Moreno, M.; Lluch, J. M.; Anglada, J. M.; Bofill, J. M. Bipyridyl Derivatives as Photomemory Devices: A Comparative Electronic-Structure Study. *Chem.—Eur. J.* **2010**, *16*, 6693−6703.

(23) Barone, V.; Palma, A.; Sanna, N. Toward a Reliable Computational Support to the Spectroscopic Characterization of Excited State Intramolecular Proton Transfer: [2,2′-Bipyridine]-3,3′-diol as a Test Case. *Chem. Phys. Lett.* **2003**, *381*, 451−457.

(24) Gelabert, R.; Moreno, M.; Lluch, J. M. Quantum Dynamics Study of the Excited-State Double-Proton Transfer in 2,2′-Bipyridyl-3,3′-diol. *Chem. Phys. Chem.* **2004**, *5*, 1372−1378.

(25) Plasser, F.; Barbatti, M.; Aquino, A. J. A.; Lischka, H. Excited-State Diproton Transfer in [2,2′-Bipyridyl]-3,3′-diol: The Mechanism Is Sequential, Not Concerted. *J. Phys. Chem. A* **2009**, *113*, 8490−8499.

(26) Marks, D.; Prosposito, P.; Zhang, H.; Glasbeek, M. Femtosecond Laser Selective Intramolecular Double-Proton Transfer in 2,2′-Bipyridyl-3,3′-diol. *Chem. Phys. Lett.* **1998**, *289*, 535−540.

(27) Zhang, H.; van der Meulen, P.; Glasbeek, M. Ultrafast Single and Double Proton Transfer in Photo-Excited [2,2′-Bipyridyl]-3,3′-diol. *Chem. Phys. Lett.* **1996**, *253*, 97−102.

(28) Toele, P.; Zhang, H.; Glasbeek, M. Femtosecond Fluorescence Anisotropy Studies of Excited-State Intramolecular Double-Proton Transfer in [2,2′-Bipyridyl]-3,3′-diol in Solution. *J. Phys. Chem. A* **2002**, *106*, 3651−3658.

(29) Prosposito, P.; Marks, D.; Zhang, H.; Glasbeek, M. Femtosecond Double Proton-Transfer Dynamics in [2,2′-Bipyridyl]-3,3′-diol in Sol−Gel Glasses. *J. Phys. Chem. A* **1998**, *102*, 8894−8902.

(30) Neuwahl, F. V. R.; Foggi, P.; Brown, R. G. Sub-picosecond and Picosecond Dynamics in the S_1 state of [2,2′-Bipyridyl]-3,3′-diol Investigated by UV−visible Transient Absorption Spectroscopy. *Chem. Phys. Lett.* **2000**, *319*, 157−163.

(31) Marks, D.; Zhang, H.; Glasbeek, M.; Borowicz, P.; Grabowska, A. Solvent Dependence of (Sub)Picosecond Proton Transfer in Photo-Excited [2,2′-Bipyridyl]-3,3′-diol. *Chem. Phys. Lett.* **1997**, *275*, 370−376.

(32) Abou-Zied, O. K. Steady-State and Time-Resolved Spectroscopy of 2,2′-Bipyridine-3,3′-diol in Solvents and Cyclodextrins: Polarity and Nanoconfinement Effects on Tautomerization. *J. Phys. Chem. B* **2010**, *114*, 1069−1076.

(33) Grabowska, A.; Borowicz, P.; Martire, D. O.; Braslavsky, S. E. Triplet States of Molecules Undergoing Internal Double-Proton Transfer in the S_1 State: 2,2′-Bipyridyl-diol and Its 5,5′-Dimethylated Derivative. *Chem. Phys. Lett.* **1991**, *185*, 206−211.

(34) Rurack, K.; Hoffmann, K.; Al-Soufi, W.; Resch-Genger, U. 2,2′-Bipyridyl-3,3′-diol Incorporated into $AlPO_4$-5 Crystals and Its Spectroscopic Properties as Related to Aqueous Liquid Media. *J. Phys. Chem. B* **2002**, *106*, 9744−9752.

(35) Nagaoka, S.; Hirota, N.; Sumitani, M.; Yoshihara, K.; Lipczynska-Kochany, E.; Iwamura, H. Investigation of the Dynamic Processes of the Excited States of o-Hydroxybenzaldehyde and Its Derivatives. 2. Effects of Structural Change and Solvent. *J. Am. Chem. Soc.* **1984**, *106*, 6913−6916.
(36) Strandjord, A. J. G.; Barbara, P. F. The Proton-Transfer Kinetics of 3-Hydroxyflavone: Solvent Effects. *J. Phys. Chem.* **1985**, *89*, 2355−2361.
(37) Abou-Zied, O. K. Investigating 2,2′-Bipyridine-3,3′-diol as a Microenvironment-Sensitive Probe: Its Binding to Cyclodextrins and Human Serum Albumin. *J. Phys. Chem. B* **2007**, *111*, 9879−9885.
(38) Abou-Zied, O. K.; Al-Hinai, A. T. Caging Effects on the Ground and Excited States of 2,2′-Bipyridine-3,3′-diol Embedded in Cyclodextrins. *J. Phys. Chem. A* **2006**, *110*, 7835−7840.
(39) De, D.; Datta, A. Modulation of Ground- and Excited-State Dynamics of [2,2′-Bipyridyl]-3,3′-diol by Micelles. *J. Phys. Chem. B* **2011**, *115*, 1032−1037.
(40) Small, D. M. *The Bile Salts*; Nair, P. P., Kritchevsky, D., Eds.; Plenum Press: New York, 1971; Vol. *1*, pp 249−256.
(41) O'Connor, C. J.; Wallace, R. G. Physico-chemical Behavior of Bile Salts. *Adv. Colloid Interface Sci.* **1985**, *22*, 1−111.
(42) Wiedmann, T. S.; Liang, W.; Kamel, L. Solubilization of Drugs by Physiological Mixtures of Bile Salts. *Pharm. Res.* **2002**, *19*, 1203−1208.
(43) Small, D. M.; Penkett, S. A.; Chapman, D. Studies on Simple and Mixed Bile Salt Micelles by Nuclear Magnetic Resonance Spectroscopy. *Biochim. Biophys. Acta* **1969**, *176*, 178−189.
(44) Funasaki, N.; Fukuba, M.; Kitagawa, T.; Nomura, M.; Ishikawa, S.; Hirota, S.; Neya, S. Two-Dimensional NMR Study on the Structures of Micelles of Sodium Taurocholate. *J. Phys. Chem. B* **2004**, *108*, 438−443.
(45) Jover, A.; Meijide, F.; Nunez, E. R.; Tato, J. V.; Mosquera, M. Aggregation Number for Sodium Deoxycholate from Steady-State and Time-Resolved Fluorescence. *Langmuir* **1997**, *13*, 161−164.
(46) Pártay, L. B.; Sega, M.; Jedlovszky, P. Molecular Aggregates in Aqueous Solutions of Bile Acid Salts. Molecular Dynamics Simulation Study. *J. Phys. Chem. B* **2007**, *111*, 9886−9896.
(47) Pártay, L. B.; Sega, M.; Jedlovszky, P. Morphology of Bile Salt Micelles as Studied by Computer Simulation Methods. *Langmuir* **2007**, *23*, 12322−12328.
(48) Gomez-Mendoza, M.; Marin, M. L.; Miranda, M. A. Dansyl Derivatives of Cholic Acid as Tools to Build Speciation Diagrams for Sodium Cholate Aggregation. *J. Phys. Chem. Lett.* **2011**, *2*, 782−785.
(49) Li, R.; Carpentier, E.; Newell, E. D.; Olague, L. M.; Heafey, E.; Yihwa, C.; Bohne, C. Effect of the Structure of Bile Salt Aggregates on the Binding of Aromatic Guests and the Accessibility of Anions. *Langmuir* **2009**, *25*, 13800−13808.
(50) Gomez-Mendoza, M.; Nuin, E.; Andreu, I.; Marin, M. L.; Miranda, M. A. Photophysical Probes to Assess the Potential of Cholic Acid Aggregates as Drug Carriers. *J. Phys. Chem. B* **2012**, *116*, 10213−10218.
(51) Amundson, L. L.; Li, R.; Bohne, C. Effect of the Guest Size and Shape on Its Binding Dynamics with Sodium Cholate Aggregates. *Langmuir* **2008**, *24*, 8491−8500.
(52) Ju, C.; Bohne, C. Dynamics of Probe Complexation to Bile Salt Aggregates. *J. Phys. Chem.* **1996**, *100*, 3847−3854.
(53) Baldridge, A.; Amador, A.; Tolbert, L. M. Fluorescence Turn On by Cholate Aggregates. *Langmuir* **2011**, *27*, 3271−3274.
(54) Megyesi, M.; Biczók, L. Berberine Alkaloid as a Sensitive Fluorescent Probe for Bile Salt Aggregates. *J. Phys. Chem. B* **2007**, *111*, 5635−5639.
(55) Rohacova, J.; Marin, M. L.; Martinez-Romero, A.; Diaz, L.; O'Connor, J. E.; Gomez-Lechon, M. J.; Donato, M. T.; Castell, J. V.; Miranda, M. A. Fluorescent Benzofurazan−Cholic Acid Conjugates for in Vitro Assessment of Bile Acid Uptake and Its Modulation by Drugs. *ChemMedChem* **2009**, *4*, 466−472.
(56) Zhong, Z.; Li, X.; Zhao, Y. Enhancing Binding Affinity by the Cooperativity between Host Conformation and Host-Guest Interactions. *J. Am. Chem. Soc.* **2011**, *133*, 8862−8865.
(57) Le Dévédec, F.; Fuentealba, D.; Strandman, S.; Bohne, C.; Zhu, X. X. Aggregation Behavior of Pegylated Bile Acid Derivatives. *Langmuir* **2012**, *28*, 13431−13440.
(58) Zhang, J.; Junk, M. J. N.; Luo, J.; Hinderberger, D.; Zhu, X. X. 1,2,3-Triazole-Containing Molecular Pockets Derived from Cholic Acid: The Influence of Structure on Host−Guest Coordination Properties. *Langmuir* **2010**, *26*, 13415−13421.
(59) Pattabiraman, M.; Kaanumalle, L. S.; Ramamurthy, V. Photoproduct Selectivity in Reactions Involving Singlet and Triplet Excited States within Bile Salt Micelles. *Langmuir* **2006**, *22*, 2185−2192.
(60) Pace, T. C. S.; Souza Júnior, S. P.; Zhang, H. T.; Bohne, C. Effect of Terbium(III) on the Binding of Aromatic Guests with Sodium Taurocholate Aggregates. *Photochem. Photobiol. Sci.* **2011**, *10*, 1568−1577.
(61) Cuquerella, M. C.; Rohacova, J.; Marin, M. L.; Miranda, M. A. Stereodifferentiation in Fluorescence Quenching within Cholic Acid Aggregates. *Chem. Commun.* **2010**, *46*, 4965−4967.
(62) Rohacova, J.; Marin, M. L.; Miranda, M. A. Complexes between Fluorescent Cholic Acid Derivatives and Human Serum Albumin. A Photophysical Approach to Investigate the Binding Behavior. *J. Phys. Chem. B* **2010**, *114*, 4710−4716.
(63) Rohacova, J.; Sastre, G.; Marin, M. L.; Miranda, M. A. Dansyl Labeling to Modulate the Relative Affinity of Bile Acids for the Binding Sites of Human Serum Albumin. *J. Phys. Chem. B* **2011**, *115*, 10518−10524.
(64) Chakraborty, A.; Chakrabarty, D.; Seth, D.; Hazra, P.; Sarkar, N. Photo-Induced Intermolecular Electron Transfer from Electron Donating Solvents to Coumarin Dyes in Bile Salt Aggregates: Role of Diffusion in Electron Transfer Reaction. *Spectrochim. Acta, Part A* **2006**, *63*, 594−602.
(65) Sen, S.; Dutta, P.; Mukherjee, S.; Bhattacharyya, K. Solvation Dynamics in Bile Salt Aggregates. *J. Phys. Chem. B* **2002**, *106*, 7745−7750.
(66) Adhikari, A.; Dey, S.; Mandal, U.; Das, D. K.; Ghosh, S.; Bhattacharyya, K. Femtosecond Solvation Dynamics in Different Regions of a Bile Salt Aggregate: Excitation Wavelength Dependence. *J. Phys. Chem. B* **2008**, *112*, 3575−3580.
(67) Hazra, P.; Chakrabarty, D.; Sarkar, N. Solvation Dynamics of Coumarin 153 in Aqueous and Non-aqueous Reverse Micelles. *Chem. Phys. Lett.* **2003**, *371*, 553−562.
(68) Seth, D.; Chakraborty, A.; Setua, P.; Sarkar, N. Interaction of Ionic Liquid with Water in Ternary Microemulsions (Triton X-100/Water/1-Butyl-3-methylimidazolium Hexafluorophosphate) Probed by Solvent and Rotational Relaxation of Coumarin 153 and Coumarin 151. *Langmuir* **2006**, *22*, 7768−7775.
(69) Demasa, J. N.; Crosby, G. A. The Measurement of Photoluminescence Quantum Yields. A Review. *J. Phys. Chem.* **1971**, *75*, 991−1024.
(70) Mandal, S.; Ghosh, S.; Banerjee, C.; Rao, V. G.; Sarkar, N. Modulation of Photophysics and Photodynamics of 1′-Hydroxy-2′-acetonaphthone (HAN) in Bile Salt Aggregates: A Study of Polarity and Nanoconfinement Effects. *J. Phys. Chem. B* **2012**, *116*, 8780−8792.
(71) Yihwa, C.; Quina, F. H.; Bohne, C. Modulation with Acetonitrile of the Dynamics of Guest Binding to the Two Distinct Binding Sites of Cholate Aggregates. *Langmuir* **2004**, *20*, 9983−9991.
(72) Wakisaka, A.; Abdoul-Carime, H.; Yamamoto, Y.; Yoshimichi, K. Non-ideality of Binary Mixtures Water−Methanol and Water−Acetonitrile from the Viewpoint of Clustering Structure. *Faraday Trans.* **1998**, *94*, 369−374.